

<https://doi.org/10.15407/ujpe70.3.206>

Y.M. AZHNIUK,¹ A.I. POGODIN,² V.V. LOPUSHANSKY,¹ M.J. FILEP,^{2,3}
V.M. KRYSHENIK,¹ I.M. VOYNAROVYCH,¹ A.V. GOMONNAI¹

¹ Institute of Electron Physics, Nat. Acad. of Sci. of Ukraine

(21, Universytetska Str., Uzhhorod 88017, Ukraine; e-mail: yu.azhniuk@gmail.com)

² Uzhhorod National University

(3, Narodna Sq., Uzhhorod 88000, Ukraine)

³ Ferenc Rákóczi II Transcarpathian Hungarian Institute

(6, Kossuth Sq., Berehovo 90200, Ukraine)

RAMAN STUDY OF VISIBLE-LIGHT PHOTOOXIDATION OF As_2S_3 : Ag GLASSES

As_2S_3 : Ag glasses (up to 10 at.% Ag) were prepared by the melt quenching. Their amorphous structure is confirmed by X-ray diffraction and Raman spectroscopy. No noticeable changes in the Raman spectra with increasing Ag content are revealed at the excitation by a 671 nm laser or by a near-bandgap laser ($\lambda_{\text{exc}} = 532$ nm) at the low power density $P_{\text{exc}} = 4$ kW/cm². Meanwhile, for the samples with Ag content above 4 at.% at the excitation by $\lambda_{\text{exc}} = 532$ nm at a higher $P_{\text{exc}} = 40$ kW/cm², new narrow peaks emerge and are clearly identified as Raman features of arsenolite (As_2O_3) formed on the As_2S_3 : Ag glass surface under the intense illumination. This is the first Raman spectroscopic evidence of the visible-light photooxidation of As_2S_3 -based glasses which previously was observed only under the illumination by ultraviolet light strongly absorbed by the surface layer leading to thermal decomposition of As_2S_3 in the illuminated area and oxidation of the vaporized arsenic atoms by oxygen from the ambient air. Most likely, the photooxidation is facilitated by the effect of silver on the glass network, reducing its rigidity, or, alternatively, the enhancement of photochemical reaction due to the plasmonic interaction of the incident light with residual ultrasmall silver nanoparticles existing in the glass sample.

Keywords: amorphous semiconductors, X-ray diffraction, Raman spectroscopy, photochemical reactions, oxidation.

1. Introduction

Amorphous arsenic trisulphide As_2S_3 is a popular semiconductor material known, first of all, due to photoinduced effects leading to drastic changes in its properties under the illumination [1–4] and making it,

along with off-stoichiometric As–S glasses, promising for applications in all-optical switching [5, 6], waveguides [5, 7], holographic gratings [6], memory devices [8], photoresists [9], substrates for surface-enhanced Raman scattering (SERS) [10], etc. Upon the illumination of amorphous As_2S_3 by ultraviolet (UV) light, photochemical reactions may occur on its surface, namely, the interaction with oxygen from the ambient air. Photooxidation of the amorphous As_2S_3 film surface under UV light was confirmed by X-ray diffraction (XRD) [11, 12], energy-dispersive X-ray spectroscopy (EDX) [11, 12], and X-ray photoelectron spectroscopy (XPS) [13]. Direct evidence for the ox-

Citation: Azhniuk Y.M., Pogodin A.I., Lopushansky V.V., Filep M.J., Kryshenik V.M., Voynarovych I.M., Gomonnai A.V. Raman study of visible-light photooxidation of As_2S_3 : Ag glasses. *Ukr. J. Phys.* **70**, No. 3, 206 (2025). <https://doi.org/10.15407/ujpe70.3.206>.

© Publisher PH “Akademperiodyka” of the NAS of Ukraine, 2025. This is an open access article under the CC BY-NC-ND license (<https://creativecommons.org/licenses/by-nc-nd/4.0/>)

idation of the amorphous As_2S_3 surface under UV laser light was demonstrated in our earlier study [14] based on the data of Raman spectroscopy.

For As_2S_3 doped with Group II metal atoms, the illumination by above-bandgap light of sufficient intensity can lead to segregation of crystallites formed with the participation of the dopant atoms and sulphur atoms from the glass network [15, 16]. These crystallites emerge as a result of a drastic photoinduced decrease in the amorphous material viscosity strongly facilitating the diffusion of atoms. Doping of As_2S_3 with Group I metals (in particular, Ag) does not reveal photoassisted segregation of Ag_2S crystalline phase; however, the interesting effect of phase separation of the glass structure into two coexisting amorphous phases (Ag-rich and Ag-poor) is reported for samples with Ag content in the interval of about 4–25 at.% [17–20]. Additional interest to amorphous Ag–As–S materials is driven by their ionic conductivity and possible applications as solid electrolytes [18, 21]. This fact is related to a higher mobility of ions (in particular, Ag^+) which could also facilitate their surface reactivity, including photochemical reactions.

Here, we intend to apply Raman spectroscopy to study the possibility of photooxidation of Ag-doped As_2S_3 glasses under the illumination by visible light. We expect Raman spectroscopy to be used simultaneously as a technique providing the source of irradiation by the excitation light and a means to detect the products of the oxidation reaction.

2. Experimental

Ag-doped As_2S_3 glass samples were prepared from pre-synthesized As_2S_3 and colloidal Ag (obtained by AgCl reduction by hydrazine chloride $\text{N}_2\text{H}_4\text{Cl}_2$ in an alkaline medium). The synthesis was carried out at 600 °C in evacuated quartz ampoules at constant stirring. The melt was kept at this temperature for 4 h and subsequently quenched rapidly at open air. Samples with silver content from 2 to 10 at.% were obtained.

To check the structure of the samples prepared, XRD measurements were carried out using a Proto Manufacturing Ltd setup with a DECTRIS MYTHEN2R 1D hybrid photon counting detector. The measurements were performed in the Bragg–Brentano geometry using Cu K_α radiation with a Ni filter.

The optical transmission spectra of $\text{As}_2\text{S}_3:\text{Ag}$ glasses were measured using a UV 1700 UV-VIS spectrophotometer (Macylab Instruments). The measurements were performed for plane-parallel polished glass samples with a thickness of 0.29–0.41 mm.

Raman scattering spectra in macroconfiguration were measured using a MDR-23 spectrometer with a cooled iDus 420 CCD detector (Andor) and a solid-state laser ($\lambda_{\text{exc}} = 671$ nm) for excitation. The laser power density on the sample surface did not exceed 1 kW/cm^2 . Micro-Raman scattering measurements were carried out using an XPloRa Plus spectrometer (Horiba Scientific) with excitation provided by a $\lambda_{\text{exc}} = 532$ nm solid-state laser with a maximal output power of 25 mW and a set of filters providing attenuation down to 0.1%. The incident laser beam was focused by a 10x objective (numeric aperture 0.25), resulting in the laser spot diameter of 2.6 μm on the sample surface. This enabled a step-wise variation of the excitation power density from 0.4 to 400 kW/cm^2 . The scattered light was detected by a cooled CCD camera. The instrumental resolution was better than 2.5 cm^{-1} . The frequency position of crystalline silicon (520.5 cm^{-1}) was used for calibration. The laser power density P_{exc} was initially reduced down to values which ensured stability of the Raman spectra and the integrity of the film surface in the laser spot. Afterwards, P_{exc} was gradually increased to observe the dynamics of laser-induced changes in the Raman spectra during the measurements. For each measurement (unless intentionally planned), a new spot was chosen on the film surface in order to exclude photo- or thermally induced changes related to previous measurements. All measurements were carried out at room temperature.

3. Results and Discussion

X-ray diffractograms of the Ag-doped As_2S_3 -based samples are shown in Fig. 1. They reveal broad smooth maxima typical of amorphous materials and practically coincide with the XRD pattern of As_2S_3 glass shown in the same figure. No signatures of any possible crystalline phases in the samples were observed.

Raman spectra of the Ag-doped As_2S_3 glasses are shown in Fig. 2. The spectra measured at the excitation by 647 nm laser light (Fig. 2, *a*), as well as those measured for $\lambda_{\text{exc}} = 532$ nm at a rather low $P_{\text{exc}} = 4$ kW/cm^2 (Fig. 2, *b*), reveal intense broad max-

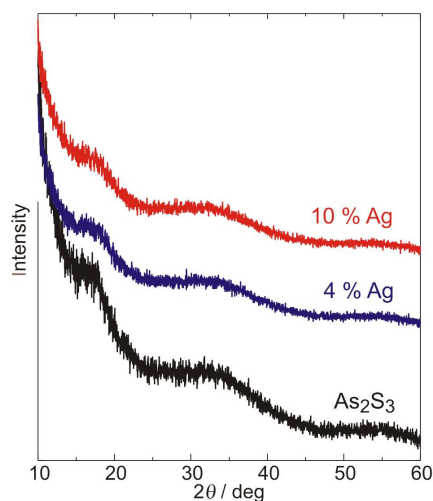


Fig. 1. XRD patterns of undoped and Ag-doped As_2S_3 glasses

ima which clearly confirm the amorphous character of the samples, exhibiting typical broad features. Amorphous arsenic sulphide As_2S_3 is characterized by a broad dominating maximum near 340 cm^{-1} (related primarily to As–S vibrations of AsS_3 (sometimes referred to as $\text{AsS}_{3/2}$) pyramidal units with minor contributions from vibrations of other structural groups) and two less intense bands near 180 cm^{-1} and 230 cm^{-1} attributed to the vibrations of homopolar As–As bonds [22–26]. Vibrations of this kind were traditionally ascribed to As-rich As_4S_4 and As_4S_3 structural groups present in the amorphous film network [22–24]; however, later targeted studies showed that these bands cannot be explained solely by the contributions of As_4S_4 and As_4S_3 units [26], and the current vision is that the homopolar As–As bonds not only belong to the cage-like As_4S_4 units, but are also formed by overcoordinated As atoms in the glass network [27].

It can be seen from Fig. 2, *a* and Fig. 2, *b* that addition of silver to As_2S_3 glass practically does not affect their Raman spectra measured at low- P_{exc} excitation. As follows from the Raman spectra of crystalline Ag_2S [31], most prominent Ag–S bond vibration frequencies are below 100 cm^{-1} while a weaker broad continuum in the interval $200\text{--}300\text{ cm}^{-1}$ could not make any noticeable contribution to the spectrum, especially at such low Ag content. In general, the addition of silver to the As_2S_3 glass composition is known to be revealed in the Raman spectra, when its content exceeds roughly 10%, exhibiting a noticeable shoulder

or even a maximum near 375 cm^{-1} [18, 29, 30]. Note that, in some studies, even for lower silver concentration (7%), a feature near 375 cm^{-1} was observed in the Raman spectra [31]. Anyway, this feature is generally considered not to be related to Ag–S bond vibrations, but rather to the vibrations of As–S bonds in AsS_3 pyramids connected by means of a S–Ag–S linkage [18, 29, 30]. In our case, as the concentration of Ag in the samples does not exceed 10 at.%, one could expect the presence and absence of the 375 cm^{-1} feature in the Raman spectra with almost equal probability. As can be seen from Fig. 2, *a* and Fig. 2, *b*, in this case, the feature corresponding to the AsS_3 pyramids linked by S–Ag–S bridges is not revealed in the spectra. Evidently, one could expect it to emerge at higher silver content in Ag–As–S glasses.

With P_{exc} increasing to 40 kW/cm^2 , the spectra of the undoped and slightly doped (4%) As_2S_3 glass remain practically unchanged, while samples with Ag content of 6% and 10% reveal a new narrow peak near 268 cm^{-1} (Fig. 2, *c*). The peak at such a frequency can be characteristic for the Raman spectrum of crystalline As_2O_3 (arsenolite, sometimes the chemical formula is written as As_4O_6), for which the T_{2g} symmetry peak at $268\text{--}269\text{ cm}^{-1}$ was reported [32]. One may suppose that the photoinduced oxidation of the As_2S_3 glass leads to a sufficient intensity of the 532 nm laser light leads to the formation of arsenolite crystallites on the sample surface. The new peak emerges in the Raman spectra of the samples under the investigation within several seconds which means that the photooxidation on the glass surface is quite fast. The photooxidation is a spatially localized effect since the laser beam was tightly focused during the measurement. Earlier, we showed that arsenolite-related features (including the peak near 268 cm^{-1}) appear in the Raman spectra of amorphous As_2S_3 under UV laser irradiation [14]. Here, the As_2O_3 signature is revealed under the illumination by much less energetic visible laser light, however, only in the presence of at least 6 at.% of silver in the sample composition.

Raman spectra measured at a lower $P_{\text{exc}} = 4\text{ kW/cm}^2$ from the same spot of the sample after the irradiation by laser light of the same wavelength $\lambda_{\text{exc}} = 532\text{ nm}$, but at a higher power density $P_{\text{exc}} = 40\text{ kW/cm}^2$ are shown in Fig. 3. The narrow As_2O_3 -related peak is clearly revealed at the background of the broad maxima of the amorphous As_2S_3 . This con-

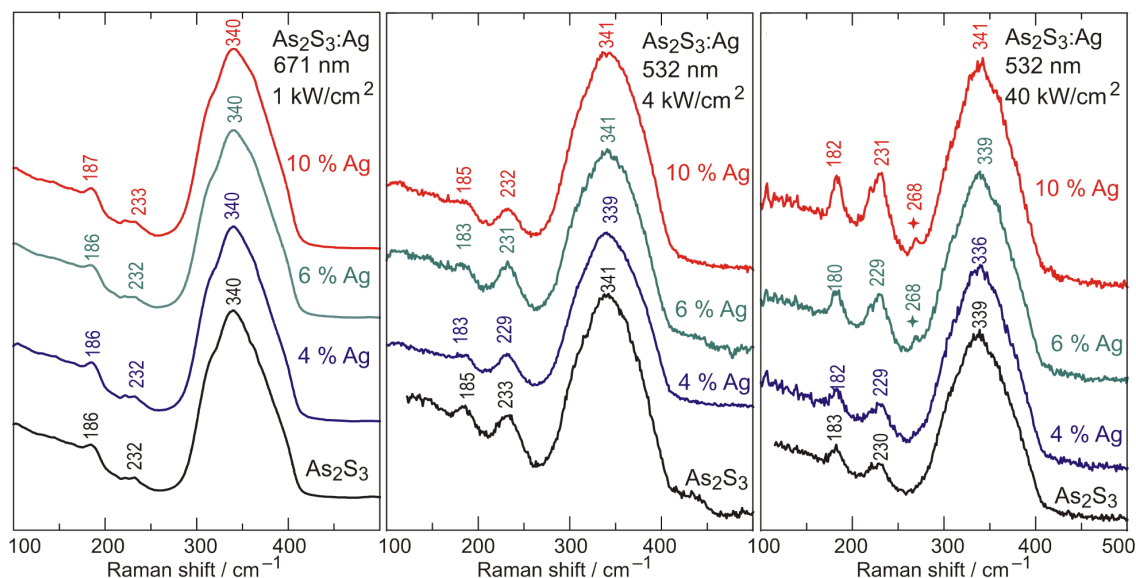


Fig. 2. Micro-Raman spectra of undoped and Ag-doped As_2S_3 -based glasses measured at the excitation with $\lambda_{\text{exc}} = 671 \text{ nm}$ at $P_{\text{exc}} = 1 \text{ kW/cm}^2$ (a) as well as with $\lambda_{\text{exc}} = 532 \text{ nm}$ at $P_{\text{exc}} = 4 \text{ kW/cm}^2$ (b) and $P_{\text{exc}} = 40 \text{ kW/cm}^2$ (c). Asterisks mark Raman peaks related to As_2O_3

firmly the irreversible character of photooxidation in the laser spot on the glass surface.

Raman spectra of the Ag-doped (10 at.%) As_2S_3 glass measured at even higher laser power density 100 kW/cm^2 (Fig. 4) reveal not only the above discussed arsenolite-related peak (in this case observed at a somewhat lower frequency 263 cm^{-1}), but also two other similar features at 365 and 555 cm^{-1} . These two peaks are also known to be characteristic of crystalline As_2O_3 , corresponding to the A_{1g} symmetry vibrations [32] and revealed in the spectra in case arsenolite is formed due to the oxidation [20]. The peak position frequencies of all the three bands are slightly shifted downward due to the sample heating in the laser spot under the high- P_{exc} illumination.

It is known that under illumination by a tightly focused above-bandgap laser beam of a rather high laser power density (in our case, $P_{\text{exc}} = 40 \text{ kW/cm}^2$) during the Raman measurement the surface of As_2S_3 glass, as well as other amorphous chalcogenides, becomes damaged with a crater-like circular pit with depth up to $500\text{--}600 \text{ nm}$ being formed in the laser spot surrounded by a rim (protrusion) with lateral size up to several micrometers [4, 15, 16, 33]. Such drastic mass transport-related changes on the glass surface are attributed not to illumination-induced heating, but to a nonthermal mechanism related

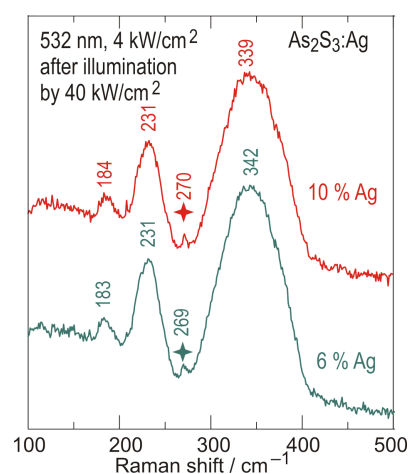


Fig. 3. Micro-Raman spectra of Ag-doped As_2S_3 glasses measured at the excitation with $\lambda_{\text{exc}} = 532 \text{ nm}$ at $P_{\text{exc}} = 4 \text{ kW/cm}^2$ after irradiation by laser light with $\lambda_{\text{exc}} = 532 \text{ nm}$ at $P_{\text{exc}} = 40 \text{ kW/cm}^2$ for 30 s. Asterisks mark Raman peaks related to As_2O_3

to photsoftening (photofluidization) [1, 3, 4, 16, 33]. Changes in local structure in amorphous chalcogenides under the illumination are treated as relaxation events around the atom, where a photon has been absorbed. As a result of non-radiative recombination, multiple bond rearrangement occurs by initiation of electron-hole pairs via transient self-trapped

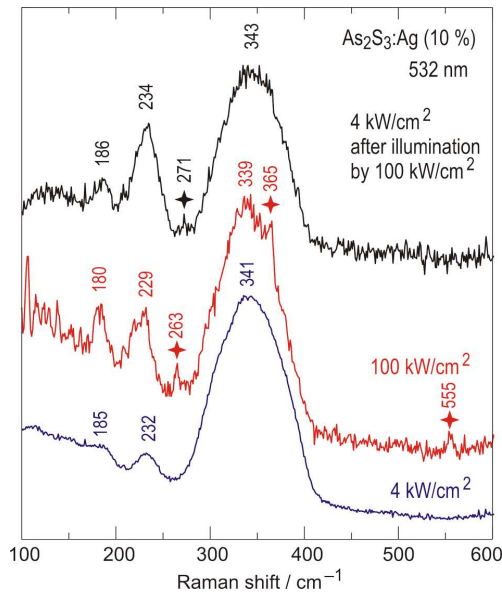


Fig. 4. Micro-Raman spectra of Ag-doped (10 at.%) As_2S_3 glasses measured at the excitation with $\lambda_{\text{exc}} = 532 \text{ nm}$ at $P_{\text{exc}} = 4 \text{ kW/cm}^2$ and $P_{\text{exc}} = 100 \text{ kW/cm}^2$ as well as at $P_{\text{exc}} = 4 \text{ kW/cm}^2$ after irradiation by laser light with $\lambda_{\text{exc}} = 532 \text{ nm}$ at $P_{\text{exc}} = 100 \text{ kW/cm}^2$ for 15 s. Asterisks mark Raman peaks related to As_2O_3

excitons [34, 35]. On the macroscopic level, the glass structure corresponds to a “saturated” dynamic state with constant physical characteristics; meanwhile, on the microscopic level, the amorphous material structure is quite unstable with perpetual bond breaking and rearrangement. Numerous acts of formation, changing, and vanishing of local and collective energy barriers which occur under the illumination result in multiple events of local fluidization [3, 34, 35]. Thereby, the photofluidization manifests itself as a drastic decrease in the material viscosity and strongly enhanced diffusion of atoms in the material under the intense illumination. Photoinduced mass transport can lead to the formation of a relief on the surface of the amorphous material [1, 4]. One could suppose that formation of arsenolite crystals in Ag-doped As_2S_3 glass under the intense illumination is related to the photoinduced material transport similarly to amorphous chalcogenides doped with Group II or Group III elements, where the photoenhanced diffusion is known to facilitate the formation of II–VI or III–V nanocrystals in the illuminated area [15, 16, 33, 36]. However, in this case, the initial glass composition does not contain oxygen (at least, in no-

ticeable amounts), therefore, it seems more appropriate to explain the observed formation of As_2O_3 crystallites under the intense illumination by thermal effect of the latter and involvement of oxygen from the ambient air. Such mechanism was proposed to explain the amorphous As_2S_3 surface photooxidation by UV light [11–14], when most of the light is absorbed by the top $0.05 \mu\text{m}$ layer of the glass sample, thereby, leading to a considerable (up to $740 \text{ }^\circ\text{C}$) heating of the material [12]. The high temperature enables breakdown of bonds in the glass network and leads to the formation of elemental arsenic $\text{As}_2\text{S}_3 \rightarrow x\text{As} + \text{As}_{2-x}\text{S}_3$, its subsequent vaporization, and oxidation by ambient oxygen $4\text{As} + 3\text{O}_2 \rightarrow 2\text{As}_2\text{O}_3$ with ambient water vapor acting as a catalyst.

As noted above, the photooxidation of amorphous arsenic trisulphide was observed only under UV light. In our case of As_2S_3 doped with a slight amount of silver, it occurs under much less energetic green light. In our experiment, its energy (2.33 eV , corresponding to $\lambda_{\text{exc}} = 532 \text{ nm}$) almost exactly matches the amorphous As_2S_3 glass optical pseudogap (absorption edge energy position at a fixed absorption level of 10^3 cm^{-1} which is 2.323 eV [37]), meaning that such quite noticeable absorption can lead to a considerable heating of the sample. However, it is definitely not sufficient to cause the formation of As_2O_3 crystallites, since it is well known that the illumination (and, consequently, heating) by visible light of similar and even higher energy (2.41 eV , $\lambda_{\text{exc}} = 514.7 \text{ nm}$) even at higher P_{exc} does not result in any noticeable photooxidation of As_2S_3 [14]. Meanwhile, doping As_2S_3 glass by silver is known to result in a red shift of the absorption edge [38]. Therefore, heating of the Ag-doped samples could be quite noticeable. Note that in our case the Ag-related shift (Fig. 5) is in a good agreement with the data for $\text{As}_2\text{S}_3\text{–Ag}_2\text{S}$ glasses reported earlier [38]. This shift leads to an increasing absorption in the sample top layer which can result in its heating in the laser spot to the temperatures sufficient to initiate the photooxidation reaction.

Note that recently we observed the formation of As_2O_3 on the surface of As_2Se_3 and Se-rich ternary As–Se–S films under illumination by visible light (514.7 nm) of sufficient power density [39]. These materials possess noticeably narrower bandgaps than As_2S_3 , therefore higher optical absorption in the green spectral range could result in the sample heat-

ing to temperatures sufficient to initiate the photooxidation reactions. Still, in our case of $\text{As}_2\text{S}_3:\text{Ag}$, the quite small (not exceeding 0.2 eV) shift of the absorption edge with doping (Fig. 5) makes the assumption of such a noticeable absorption increase (and, consequently, a strong heating of the sample) merely due to the edge shift somewhat doubtful.

From recent studies it is known that the presence of certain intentionally or unintentionally introduced dopants can strongly facilitate photooxidation reactions on the surface of crystalline [40] or glassy [41] As_2S_3 . One should also note that earlier XPS [44] and XRD [45, 46] studies reported photooxidation under visible light for Ag/ As_2S_3 bilayer structures, where silver was migrating into the As_2S_3 layer due to photodoping. Moreover, especially in the presence of water from the ambient air, the photooxidation can also lead to the formation of not only As_2O_3 , but also compounds with arsenic in a higher oxidation state (+5) [40, 41]. In particular, for orpiment (crystalline As_2S_3) the photoinduced formation of arsenate $\text{As}_2\text{O}_3^{3-}$ ions was strongly assisted by the presence of Pb [40]. Likewise, arsenates are formed under the illumination (even by visible light) on the surface of As_2S_3 -based glasses with a rather noticeable (above 14 %) amount of bismuth [41].

On the other hand, for a related amorphous chalcogenide As_2Se_3 , it is known that doping with metals prevents (in case of Cu dopant) or inhibits (doping with Ag) the photooxidation reactions on the surface [47]. Threshold optical intensity for the formation of As_2O_3 microcrystals in Ag-doped As_2Se_3 glasses was confirmed to be much higher than that for undoped As_2Se_3 [38]. These results disagree with our data; evidently, the incorporation of silver in the arsenic chalcogenide glass network goes in a different manner for As_2S_3 and As_2Se_3 . Maybe, some issues could be clarified by studies of Ag-doped As–Se–S glasses, but currently available Raman studies of such materials did not reveal photooxidation effects either due to a much less energetic light being used for the excitation [48, 49], or because of the absence of the arsenolite peaks in the spectra [50, 51].

Another possibility could be considered in case if part of silver had not been initially dissolved in the glass, incorporating in its structural network, but had remained in the residual form of colloidal nanoparticles (which could avoid being detected by XRD due

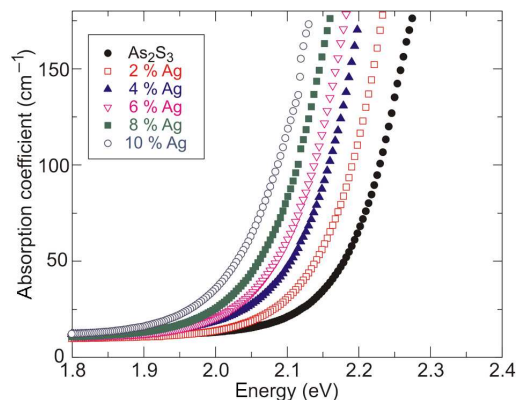


Fig. 5. Optical absorption spectra of undoped and Ag-doped As_2S_3 glasses measured at room temperature

to their ultrasmall size). In such case, the interaction of the incident laser light with silver nanoparticles (for which the plasmonic resonance frequency is not far from the green spectral range [52]) could facilitate the surface oxidation of As_2S_3 in a way similarly to the plasmon-polariton interaction-related enhancement of photodiffusion of silver in As_2S_3 [53] or SERS recently reported for chalcogenide glass-based structures [54, 55].

As mentioned above, recent studies performed for arsenic sulphide doped with Pb [40] or Bi [41] reported the photoinduced formation of arsenates, however, in our case no Raman signatures of arsenate ions were observed. Hence, for Ag-doped As_2S_3 illumination by 532 nm light, at least for the P_{exc} range under investigation, does not result in the oxidation of arsenic to its highest (+5) oxidation state.

Strictly speaking, since the experiment was performed on air, a possibility of photoinduced reactions of arsenic or sulphur on the sample surface with nitrogen should also be considered. To our knowledge, the existence of crystalline arsenic nitride was first reported only recently [56] where this compound was obtained under a very high pressure (300,000 times the atmospheric pressure) and temperature (1200 °C). In our case, such a possibility can definitely be excluded. We did not find any coincidence of the new peaks emerging in our experiment with those known for S_4N^- and S_3N^- ions [57] or cyclic S_4N_3^+ cations [58]. Therefore, under such conditions, one can hardly expect a possibility of photochemical reaction of amorphous arsenic sulphide with nitrogen.

4. Conclusions

Ag-doped As_2S_3 glasses with silver content up to 10 at.% are prepared by the melt quenching technique. Their amorphous structure was clearly confirmed by XRD measurements and Raman spectra.

Raman measurements performed under the excitation by a 671 nm laser or by a near-bandgap laser $\lambda_{\text{exc}} = 532$ nm at low power density $P_{\text{exc}} = 4$ kW/cm² did not reveal noticeable changes in the spectra with increasing the silver content. Meanwhile, for the samples with Ag content above 4 at.% under the excitation by $\lambda_{\text{exc}} = 532$ nm at a higher $P_{\text{exc}} = 40$ kW/cm², a new narrow peak emerges near 268 cm⁻¹ that was not revealed at a lower P_{exc} . This peak retains in the Raman spectra measured at a reduced P_{exc} after the irradiation at an increased power density, confirming the irreversible character of the photoinduced transformation having initiated the new peak appearance. At an even higher $P_{\text{exc}} = 100$ kW/cm², the appearance of this peak is accompanied by new narrow peaks near 365 and 555 cm⁻¹. The new peaks are clearly identified as Raman features of arsenolite (As_2O_3) which is formed on the As_2S_3 :Ag glass surface under an intense illumination. Photooxidation of amorphous As_2S_3 was previously known to occur under UV light strongly absorbed by the surface layer leading to the thermal decomposition of As_2S_3 in the illuminated area and oxidation of the vaporized arsenic atoms by oxygen from the ambient air [11–14, 38]. To our knowledge, this is the first Raman-based evidence of the visible-light photooxidation of As_2S_3 -based glasses. It is definitely enabled by the presence of silver in the glass composition. It seems less reasonable to relate this effect simply to the increasing absorption of the 532-nm laser light by the surface layer of the glass with increasing Ag content. More likely, the photooxidation is facilitated by the effect of silver on the glass network, reducing its rigidity, or, alternatively, the enhancement of photochemical reaction due to the plasmonic interaction of the incident light with residual ultrasmall silver nanoparticles existing in the glass sample. Additional studies are required to clarify the mechanism of the effect of silver facilitating the photooxidation reaction on the As_2S_3 glass surface.

The authors are indebted to V.O. Yukhymchuk for valuable assistance and discussion. This work was

supported by the “Advanced Science in Ukraine” grant No. 2023.03/0013 from National Research Foundation of Ukraine.

1. K. Tanaka. Photoinduced deformations in chalcogenide glasses. In *Amorphous Chalcogenides: Advances and Applications*. Edited by R.P. Wang (Pan Stanford Publishing, 2014), p. 59 [ISBN: 978-0-429-07429-5].
2. K. Tanaka, K. Shimakawa. *Amorphous chalcogenide semiconductors and related materials* (Springer, 2021) [ISBN: 978-3-030-69598-9].
3. S.N. Yannopoulos. Athermal photoelectronic effects in non-crystalline chalcogenides: Current status and beyond. In *The World Scientific Reference of Amorphous Materials*. Edited by A.V. Kolobov, K. Shimakawa (World Scientific, 2021), p. 251 [ISBN: 978-981-12-1594-0].
4. Y. Azhniuk, V. Kryshenik, M. Rahaman, V. Loya, V. Lopushansky, A.V. Gomonnai, D.R.T. Zahn. Mass transport in amorphous As_2S_3 films due to directional light scattering under illumination by an oblique tightly focused beam. *J. Non-Cryst. Solids* **576**, 121269 (2022).
5. B.J. Eggleton, B. Luther-Davies, K. Richardson. Chalcogenide photonics. *Nature Photonics* **5**, 141 (2011).
6. V.M. Kryshenik, Yu.M. Azhniuk, V.S. Kovtunencko. All-optical patterning in azobenzene polymers and amorphous chalcogenides. *J. Non-Cryst. Solids* **512**, 112 (2019).
7. L. Li, H. Lin, S. Qiao, Y. Zou, S. Danto, K. Richardson, J.D. Musgraves, N. Lu, J. Hu. Integrated flexible chalcogenide glass photonic devices. *Nature Photonics* **8**, 643 (2014).
8. V.M. Kryshenik. Dynamic photoinduced changes of optical characteristics and effect of optical memory in amorphous As–S film-based waveguides. *J. Non-Cryst. Solids* **585**, 121528 (2022).
9. A. Kovalskiy, J. Cech, M. Vlcek, C.M. Waits, M. Dubey, W.R. Heffner, H. Jain, Chalcogenide glass e-beam and photoresists for ultrathin grayscale patterning. *J. Micro/Nanolith. MEMS MOEMS* **8**, 043012 (2009).
10. L. Su, C.J. Rowlands, S.R. Elliott. Nanostructures fabricated in chalcogenide glass for use as surface-enhanced Raman scattering substrates. *Opt. Lett.* **34**, 1645 (2009).
11. P.J. Allen, B.R. Johnson, B.J. Riley. Photo-oxidation of thermally evaporated As_2S_3 thin films. *J. Optoelectron. Adv. Mater.* **7**, 1759 (2005).
12. P. Knotek, M. Vlcek, M. Kincl, L. Tichy. On the ultraviolet light induced oxidation of amorphous As_2S_3 film. *Thin Solid Films* **520**, 5472 (2012).
13. A. Kovalskiy, M. Vlcek, K. Palka, J. Buzek, J. York-Winegar, J. Oelgoetz, R. Golovchak, O. Shpotyuk, H. Jain, Structural origin of surface transformations in arsenic sulfide thin films upon UV-irradiation. *Appl. Surf. Sci.* **394**, 604 (2017).
14. Y. Azhniuk, D. Solonenko, V. Loya, I. Grytsyshche, V. Lopushansky, A.V. Gomonnai, D.R.T. Zahn. Raman evidence for surface oxidation of amorphous As_2S_3 thin films un-

- der ultraviolet irradiation. *Appl. Surf. Sci.* **467–468**, 119 (2019).
15. Yu.M. Azhniuk, V.M. Dzhagan, D. Solonenko, A. Mukherjee, V.Yu. Loya, I.V. Grytsyshche, V.V. Lopushansky, A.V. Gomonnai, D.R.T. Zahn, Laser annealing-induced formation of CdS nanocrystals in Cd-doped amorphous As₂S₃ thin films. *Phys. Status Solidi B* **256**, 1800298 (2019).
 16. Y.M. Azhniuk, V.V. Lopushansky, V.Yu. Loya, V.M. Kryshenik, V.M. Dzhagan, A.V. Gomonnai, D.R.T. Zahn. Raman study of laser-induced formation of II–VI nanocrystals in zinc-doped As–S(Se) films. *Appl. Nanosci.* **10**, 4831 (2020).
 17. M. Ohta, M. Tsutsumi, F. Izumi, S. Ueno. Phase separation and structural change accompanying the introduction of silver to arsenic trisulphide glass. *J. Mater. Sci.* **17**, 2431 (1982).
 18. F. Kyriazis, A. Chrissanthopoulos, V. Dracopoulos, M. Krbal, T. Wagner, M. Frumar, S.N. Yannopoulos, Effect of silver doping on the structure and phase separation of sulfur-rich As–S glasses: Raman and SEM studies. *J. Non-Cryst. Solids* **355**, 2010 (2009).
 19. Th.Ch. Hasapis, K.S. Andrikopoulos, E. Hatzikraniotis, V. Dracopoulos, T. Wagner, S.N. Yannopoulos, K.M. Paraskevopoulos, Vibrational properties of silver-doped arsenic chalcogenide bulk glasses. *AIP Conf. Proc.* **1203**, 283 (2010).
 20. K.S. Andrikopoulos, J. Arvanitidis, V. Dracopoulos, D. Christofilos, T. Wagner, S.N. Yannopoulos. Nanoindentation and Raman studies of phase-separated Ag–As–S glasses. *Appl. Phys. Lett.* **99**, 171911 (2011).
 21. M. Frumar, T. Wagner. Ag doped chalcogenide glasses and their applications. *Curr. Opin. Solid State Mater. Sci.* **7**, 117 (2003).
 22. D.G. Georgiev, P. Boolchand, K.A. Jackson, Intrinsic nanoscale phase separation of bulk As₂S₃ glass. *Phil. Mag.* **83**, 2941 (2003).
 23. P. Chen, C. Holbrook, P. Boolchand, D.G. Georgiev, K.A. Jackson, M. Micoulaut. Intermediate phase, network demixing, boson and floppy modes, and compositional trends in glass transition temperatures of binary As_xS_{1–x} system. *Phys. Rev. B* **78**, 224208 (2008).
 24. R. Holomb, M. Veres, V. Mitsa. Ring-, branchy-, and cage-like As_nS_m nanoclusters in the structure of amorphous semiconductors: *ab initio* and Raman study. *J. Optoelectron. Adv. Mater.* **11**, 917 (2009).
 25. R. Golovchak, O. Shpotyuk, J.S. McCloy, B.J. Riley, C.F. Windisch, S.K. Sundaram, A. Kovalskiy, H. Jain, Structural model of homogeneous As–S glasses derived from Raman spectroscopy and high-resolution XPS. *Phil. Mag.* **90**, 4489 (2010).
 26. S.N. Yannopoulos, K.S. Andrikopoulos, D.Th. Kastrissios, G.N. Papatheodorou. Origin of photoinduced defects in glassy As₂S₃ under band gap illumination studied by Raman scattering: A revisory approach. *Phys. Status Solidi B* **249**, 2005 (2012).
 27. D. Tsiulyanu, M. Veres, R. Holomb, M. Ciobanu. Raman scattering evidence on the correlation of middle range order and structural self-organization of As–S–Ge glasses in the intermediate phase region, *J. Non-Cryst. Solids* **609** (2023) 122255. *J. Non-Cryst. Solids* **609**, 122255 (2023).
 28. O. Alekperov, Z. Jahangirli, R. Paucar. First-principles lattice dynamics and Raman scattering in ionic conductor β-Ag₂S. *Phys. Status Solidi B* **253**, 2049 (2016).
 29. T. Wágner, Mir. Vlček, S.O. Kasap, Mil. Vlček, M. Frumar. Changing the composition of Ag–As–S amorphous films using photo-induced solid state reaction. *J. Non-Cryst. Solids* **284**, 168 (2001).
 30. M. Krbal, T. Wagner, T. Kohoutek, P. Nemeč, J. Orava, M. Frumar. The comparison of Ag–As₃₃S₆₇ films prepared by thermal evaporation (TE), spin-coating (SC) and a pulsed laser deposition (PLD). *J. Phys. Chem. Solids* **68**, 953 (2007).
 31. A. Stronski, L. Revutska, A. Meshalkin, O. Paiuk, E. Achimova, A. Korchovyi, K. Shportko, O. Gudymenko, A. Priscar, A. Gubanova, G. Triduh. Structural properties of Ag–As–S chalcogenide glasses in phase separation region and their application in holographic grating recording. *Opt. Mater.* **94**, 393 (2019).
 32. S.J. Gilliam, C.N. Merrow, S.J. Kirkby, J.O. Jensen, D. Zeroka, A. Banerjee. Raman spectroscopy of arsenolite: crystalline cubic As₄O₆. *J. Solid State Chem.* **173**, 54 (2003).
 33. Yu.M. Azhniuk, D. Solonenko, V.Yu. Loya, V.M. Kryshenik, V.V. Lopushansky, A. Mukherjee, A.V. Gomonnai, D.R.T. Zahn, Flexoelectric and local heating effects on CdSe nanocrystals in amorphous As₂Se₃ films. *Mater. Res. Expr.* **6**, 095913 (2019).
 34. H. Fritzsche. Photo-induced fluidity of chalcogenide glasses. *Solid State Commun.* **99**, 153 (1996).
 35. K. Tanaka, K. Shimakawa. Mechanisms of photoinduced fluidity in chalcogenide glasses: Molecular orbital analyses. *J. Non-Cryst. Solids* **481**, 579 (2018).
 36. Y. Azhniuk, V. Dzhagan, D. Solonenko, V. Loya, I. Grytsyshche, V. Lopushansky, A.V. Gomonnai, D.R.T. Zahn, In-doped As₂Se₃ thin films studied by Raman and X-ray photoelectron spectroscopies. *Appl. Surf. Sci.* **471**, 943 (2019).
 37. I.P. Studenyak, M. Kranjčec, M.M. Pop. Urbach absorption edge and disordering processes in As₂S₃ thin films. *J. Non-Cryst. Solids* **357**, 3866 (2011).
 38. O.I. Shpak, M.M. Pop, I.I. Shpak, I.P. Studenyak. Refractometric studies of chalcogenide glasses in Ag–As–S system. *Opt. Mater.* **35**, 297 (2012).
 39. Y. Azhniuk, V. Lopushansky, V. Loya, D. Solonenko, V. Kryshenik, I.M. Voynarovych, A.V. Gomonnai, D.R.T. Zahn. Raman evidence for the oxidation of amorphous arsenic chalcogenide film surfaces under visible light. *Mater. Res. Expr.* **11**, 046405 (2024).
 40. F.T.H. Broers, K. Janssens, J. Nelson Weker, S.M. Webb, A. Mehta, F. Meirer, K. Keune. Two pathways for the degradation of orpiment pigment (As₂S₃) found in paintings. *J. Amer. Chem. Soc.* **145**, 8847 (2023).

41. Y. Azhniuk, V. Lopushansky, S. Hasynets, V. Kryshenik, A.V. Gomonnai, D.R.T. Zahn. Photoinduced transformations in $(As_{1-x}Bi_xS_3)$ glass observed by Raman spectroscopy. *J. Raman Spectrosc.* **55**, 637 (2024).
42. K. Keune, J. Mass, F. Meirer, C. Pottasch, A. van Loon, A. Hull, J. Church, E. Pouyet, M. Cotte, A. Mehta. Tracking the transformation and transport of arsenic sulfide pigments in paints: synchrotron-based X-ray micro-analyses. *J. Anal. At. Spectrom.* **30**, 813 (2015).
43. M. Vermeulen, J. Sanyova, K. Janssens, G. Nuyts, S. De Meyer, K. De Wael. The darkening of copper- or lead-based pigments explained by a structural modification of natural orpiment: a spectroscopic and electrochemical study. *J. Anal. At. Spectrom.* **32**, 1331 (2017).
44. A. Kovalskiy, A. Ganjoo, S. Khalid, H. Jain. Combined high-resolution XPS and EXAFS study of Ag photodissolution in $a-As_2S_3$ thin film, *J. Non-Cryst. Solids* **356**, 2332 (2010).
45. M. Popescu, F. Sava, A. Lorinczi, A. Velea, M. Leonovici, S. Zamfira. Silver/amorphous As_2S_3 heterostructure. *J. Optoelectron. Adv. Mater.* **11**, 1586 (2009).
46. F. Sava, M. Popescu, A. Lörinczi, A. Velea. Possible mechanism of Ag photodiffusion in $a-As_2S_3$ thin films. *Phys. Status Solidi B* **250**, 999 (2013).
47. K. Ogusu, Y. Hosokawa, S. Maeda, M. Minakata, H. Li. Photo-oxidation of As_2Se_3 , $Ag-As_2Se_3$, and $Cu-As_2Se_3$ chalcogenide films. *J. Non-Cryst. Solids* **351**, 3132 (2005).
48. A.V. Stronski, M. Vlček, A.I. Stetsun, A. Sklenář, P.E. Shepeliavii. Raman spectra of Ag- and Cu- photodoped chalcogenide films. *Semicond. Phys. Quantum Electron. Optoelectron.* **2** (2), 63 (1999).
49. J. Tasseva, R. Todorov, Tz. Babeva, K. Petkov. Structural and optical characterization of Ag photo-doped thin $As_{40}S_{60-x}Se_x$ films for non-linear applications. *J. Opt.* **12**, 065601 (2010).
50. J. Orava, T. Wagner, M. Krbal, T. Kohoutek, Mil. Vlcek, L. Benes, E. Kotulanova, P. Bezdička, P. Klapetek, M. Frumar. Selective wet-etching of amorphous/crystallized $Ag-As-S$ and $Ag-As-S-Se$ chalcogenide thin films. *J. Phys. Chem. Solids* **68**, 1008 (2007).
51. K.O. Čajko, M. Dimitrievska, D.L. Sekulić, D.M. Petrović, S.R. Lukić-Petrović. Ag-doped $As-S-Se$ chalcogenide glasses: a correlative study of structural and dielectrical properties. *J. Mater. Sci.: Mater. Electron.* **32**, 6688 (2021).
52. I.M. Bolesta, M.M. Vakiv, V.G. Haiduchok, I.I. Kolych, A.A. Kushnir, I.M. Rovetsky, Yu.M. Furgala. Plasmon absorption by silver nanoparticles on $LiNbO_3$ surface. *Ukr. J. Phys.* **62**, 39 (2017).
53. I. Indutnyi, V. Mynko, M. Sopinsky, P. Lytvyn. Impact of surface plasmon polaritons on silver photodiffusion into As_2S_3 film. *Plasmonics* **16**, 181 (2021).
54. V.O. Yukhymchuk, V.M. Rubish, V.M. Dzhagan, O.M. Hreshchuk, O.F. Isaieva, N.V. Mazur, M.O. Durkot, A.A. Kryuchyn, V.K. Kyrylenko, V.M. Novichenko, V.V. Kremenyskyi, Z.V. Maksimenko, M.Ya. Valakh. Surface-enhanced Raman scattering of As_2S_3 and Se thin films formed on Au nanostructures. *Semicond. Phys. Quantum Electron. Optoelectron.* **26**, 49 (2023).
55. I.Z. Indutnyi, V.O. Yukhymchuk, V.I. Mynko, S.V. Mamykin, N.V. Mazur, O.F. Isaieva, V.M. Dzhagan, V.A. Danko, V.S. Yefanov, A.A. Korchovy, P.M. Lytvyn. Shape effect of laterally ordered nanostructures on the efficiency of surface-enhanced Raman scattering. *Ukr. J. Phys.* **69**, 11 (2024).
56. M. Ceppatelli, D. Scelta, M. Serrano-Ruiz, K. Dziubek, M. Morana, V. Svitlyk, G. Garbarino, T. Poręba, M. Mezouar, M. Peruzzini, R. Bini. Single-bonded cubic AsN from high-pressure and high-temperature chemical reactivity of arsenic and nitrogen. *Angew. Chem. Int. Ed.* **66**, e202114191 (2022).
57. T. Chivers, C. Lau. Raman spectroscopic identification of the S_4N^- and S_3N^- ions in blue solutions of sulfur in liquid ammonia. *Inorg. Chem.* **21**, 453 (1982).
58. S.H. Aryal, K.M. Page, S.M. Hyatt, R. Liu. Reassignment of fundamental vibrational modes of cyclic S_4N_3 cation. *Spectrochim. Acta A* **56**, 851 (2000).

Received 01.10.24

Ю.М. Ажнюк, А.І. Погодін,
В.В. Лопушанський, М.Й. Філеп,
В.М. Кришеник, І.М. Войнарович, О.В. Гомоннай

РАМАНІВСЬКЕ ДОСЛІДЖЕННЯ ФОТООКИСЛЕННЯ СКЛА $As_2S_3 : Ag$ ПІД ДІЄЮ ВИДИМОГО СВІТЛА

Зразки скла $As_2S_3 : Ag$ (до 10 ат.% Ag) отримано охолодженням з розплаву. Їхню аморфну структуру підтверджено даними дифракції рентгенівських променів і раманівської спектроскопії. При збудженні світлом лазера з довжиною хвилі $\lambda_{exc} = 671$ нм помітних змін у раманівських спектрах при зростанні вмісту Ag не виявлено, так само як і при збудженні лазером з $\lambda_{exc} = 532$ нм з низькою густиною потужності $P_{exc} = 4$ кВт/см². Тоді як для зразків із вмістом Ag понад 4 ат.% при збудженні $\lambda_{exc} = 532$ нм з вищою $P_{exc} = 40$ кВт/см² у спектрі з'являються нові вузькі піки, чітко ідентифіковані як раманівські смуги арсеноліту (As_2O_3), який утворюється на поверхні скла $As_2S_3 : Ag$ при інтенсивному опроміненні. Це перше свідчення фотоокислення скла на основі As_2S_3 під дією видимого світла, отримане методом раманівської спектроскопії. Раніше подібне спостерігалось тільки під дією ультрафіолетового світла, яке сильно поглиналося поверхневим шаром скла й вело до термічного розкладу As_2S_3 в освітленій області й окислення випаруваних атомів арсену киснем повітря. Очевидно, фотоокисленню сприяє наявність срібла у структурі скла, що зменшує його жорсткість, або ж підсилення фотохімічної реакції внаслідок плазмонної взаємодії падаючого світла з залишковими ультрамалими наночастинками срібла, присутніми у склоподібному зразку.

Ключові слова: аморфні напівпровідники, дифракція рентгенівських променів, раманівська спектроскопія, фотохімічні реакції, окислення.